Resonance Raman Characterization of H(M200)L Mutant Reaction Centers from *Rhodobacter capsulatus*. Effects of Heterodimer Formation on the Structural and Electronic Properties of the Cofactors†

Vaithianathan Palaniappan and David F. Bocian*

Department of Chemistry, University of California, Riverside, California 92521-0403

Received March 24, 1995; Revised Manuscript Received June 19, 1995⊗

ABSTRACT: Resonance Raman (RR) spectra are reported for photosynthetic reactions centers (RCs) from the H(M200)L mutant of *Rhodobacter capsulatus*. In this mutant, the histidine residue which ligates the M-side bacteriochlorophyll (BCh) of the special pair primary donor (P) of wild-type RCs is replaced by a noncoordinating leucine. This results in the formation of a heterodimer primary donor (D) in which a bacteriopheophytin (BPh) replaces the M-side BCh. The RR data for the H(M200)L mutant were acquired at a large number of excitation wavelengths which span the B, Q_x, and Q_y absorption bands of the various bacteriochlorin cofactors in the RC. For comparison, spectra were also acquired for wild-type RCs at the same excitation wavelengths. The RR data obtained for the mutant indicate that heterodimer formation induces a variety of changes in the structural and electronic properties of the cofactors in the RC. These perturbations extend beyond the primary donor and include one of the two accessory BChs. Collectively, the RR studies indicate the following: (1) The structure of the single BCh cofactor in D [D_L(BCh)] is different from that of either of the two BChs in P. However, D_L(BCh) is more similar to P_L than to P_M. The P_M cofactor is conformationally more distorted than either P_L or D_L(BCh). (2) The structure of the BPh cofactor in D [D_M(BPh)] is similar to that of the other two BPhs in the RC. However, the frequency of the C_9-keto carbonyl mode of D_M(BPh) is anomalously low (1678 cm^{-1}), as is also the case for P_M. The vibrational characteristics of the C_9-keto carbonyl vibrations of D_M(BPh)/P_M versus D_L(BCh)/P_L are consistent the notion that dielectric effects govern the frequency of the mode and that the effective dielectric constant is different on the L- versus M-sides of the primary donor. (3) Heterodimer formation perturbs the structural and electronic properties of one of the two accessory BChs (most likely BCh_L) in the RC. These perturbations are manifested as upshifts in the ring skeletal-mode frequencies and a blue-shift in the Q_x absorption band (from 600 to 580 nm). The fact that heterodimer formation perturbs one of the accessory BChs suggests that global structural rearrangements occur in the protein matrix when the ligand to a cofactor in the primary donor is removed. (4) For both the H(M200)L mutant and wild-type RCs, oxidation of the primary donor significantly affects the RR cross section of the carotenoid. This effect indicates strong primary donor−carotenoid interactions and suggest that ultrafast energy transfer (100 fs or less) occurs between these cofactors. The fact that the RR cross section of the carotenoid is sensitive to these interactions opens new avenues for investigating the S_2 excited-state dynamics of carotenoids in RCs.

The primary electron-transfer processes in bacterial photosynthesis occur in a membrane protein complex known as the reaction center (RC)[1] (Kirmaier & Holten, 1987; Boxer et al., 1989; Deisenhofer & Michel, 1989a; Feher, 1989; Friesner & Won, 1989; Breton & Verméglio, 1992; Deisenhofer & Norris, 1993). The primary electron donor in RCs is a dimer [the special pair (P)] of bacteriochlorophyll (BCh) molecules; the primary acceptor is a bacteriopheophytin (BPh) molecule. RCs also contain one other BPh, two monomeric BChs, a carotenoid, and a non-heme iron center. X-ray crystallographic studies of RCs from *Rhodobacter sphaeroides* and *Rhodopseudomonas viridis* indicate that P, the accessory BChs, and the BPhs are arranged in the L and M polypeptides such that the macroscopic symmetry is approximately C_2 (Deisenhofer et al., 1985; Chang et al., 1986; Allen et al., 1986; Yeates et al., 1988; Deisenhofer & Michel, 1989b; El-Kabbani et al., 1991; Ermler et al., 1994; Deisenhofer et al., 1995). The Mg(II) ions of the two BChs in P and the two accessory BChs are each ligated to a histidine residue (Ermler et al., 1994). This ligation conserves the approximate C_2 symmetry in the RC. This symmetry is broken, however, by inequivalences at other positions in the primary amino acid sequence of the L versus M subunits. These asymmetries are presumably responsible for the fact that electron transfer occurs only down the L branch (Kirmaier et al., 1985).

The symmetry of P can be dramatically altered by replacing either of the ligating histidines with a noncoordinating leucine. This modification results in the formation of a heterodimer primary donor (D) in which one of the two BChs is replaced by a BPh (Bylina & Youvan, 1988;

† This work was supported by Grant GM39781 (D.F.B.) from the National Institute of General Medical Sciences.

⊗ Abstract published in *Advance ACS Abstracts,* August 15, 1995.

[1] Abbreviations: BCh, bacteriochlorophyll; BPh, bacteriopheophytin; D, the heterodimer primary donor in H(M200)L mutant reaction centers; FT-IR, Fourier-transform infrared; L and M, light and medium polypeptides of the reaction center; P, the special pair primary donor in wild-type reaction centers; Q_A, quinone; RCs, reaction centers; RR, resonance Raman.

0006-2960/95/0434-11106$09.00/0

Schenck et al., 1990; McDowell et al., 1991a,b). Owing to the inherent asymmetry in D, its electronic properties and spectral signatures are significantly different from those of P (Bylina & Youvan, 1988; Breton et al., 1989; Bylina et al., 1990; Dimagno et al., 1990; Hammes et al., 1990; Huber et al., 1990; Frank et al., 1993). The electron-transfer kinetics of heterodimer RCs are also different from those wild-type; however, the unidirectionality of electron transfer is retained in both L- and M-side heterodimer mutants (Kirmaier et al., 1988, 1989; McDowell et al., 1990, 1991a,b; Laporte et al., 1993).

In order to determine how genetic modifications influence the electronic and photophysical properties RCs, it is necessary to know how these modifications affect the structure of the bacteriochlorin cofactors. In cases where the replacement does not involve a protein residue in direct contact with a cofactor, it is perhaps reasonable to assume that the structure of the cofactor is similar to that in wild-type RCs. On the other hand, replacements such as those that lead to heterodimer formation could result in more significant structural perturbations. At this time, preliminary X-ray crystallographic data are available for heterodimer RCs from *Rb. sphaeroides*; however, the resolution (3−4 Å) is not sufficiently high to elucidate the detailed structure of the cofactors (Chirino et al., 1994). Vibrational spectroscopy provides an attractive alternative for addressing this issue. The vibrational signatures of the ring-skeletal and carbonyl modes reflect the conformation of the bacteriochlorin macrocycle and the interactions between the conjugating substituent groups and the protein matrix (Lutz, 1984; Lutz & Robert, 1988; Robert, 1990; Peloquin et al., 1990a,b, 1991; Lutz & Mäntele, 1991; Mattioli et al., 1991, 1994; Palaniappan & Bocian, 1992, 1995; Palaniappan et al., 1993; Leonhard & Mäntele, 1993; Nabedryk et al., 1992, 1993; Wachtveitl et al., 1993; Jones et al., 1994). In the case of heterodimer RCs, only limited vibrational data are currently available. Our group reported resonance Raman (RR) spectra of the M-side heterodimer mutant, H(M200)L, from *Rhodobacter capsulatus* (Peloquin et al., 1990b). The principal aim of this study was to probe the structure of the cofactors in D via characterization of the ring-skeletal modes. This effort was only partially successful due to the fact that RR data were acquired at a limited number of excitation wavelengths. Nabedryk et al. (1992) examined the Fourier-transform infrared (FT-IR) spectra of H(M200)L mutant RCs as well as those from the L-side heterodimer mutant H(L173)L. The FT-IR studies focused primarily on cofactor−protein interactions as reflected by the keto carbonyl stretching vibrations of the bacteriochlorins in D. Although certain bands associated with these modes were assigned, the full complement of C_9-keto and C_{2a}-acetyl carbonyl stretches ($\nu C_9{=}O$ and $\nu C_{2a}{=}O$) was not identified.

In this paper, we report a detailed RR study of H(M200)L mutant RCs from *Rb. capsulatus*. Unlike our earlier study of this mutant (Peloquin et al., 1990b), the RR data reported herein were obtained at a large number of excitation wavelengths which span the B, Q_x, and Q_y absorption bands of the different pigments. For comparison, spectra were also obtained for wild-type RCs. For the mutant and wild-type, data were acquired for both chemically reduced (Q_A^-) and oxidized (D^+ or P^+) RCs. The work focuses on the high-frequency (1400−1750 cm^{-1}) ring-skeletal and carbonyl vibrations of the bacteriochlorin cofactors. These modes have been previously assigned for BCh and BPh in solution and in wild-type RCs (Donohoe et al., 1988; Lutz & Robert, 1988; Robert, 1990; Lutz & Mäntele, 1991; Palaniappan et al., 1993; Diers & Bocian, 1994). Collectively, the RR data provide a more detailed picture of the structural and electronic properties of the primary donor in both the H(M200)L mutant and wild-type RCs. The data also provide new insights into the effects of heterodimer formation on the other cofactors in the protein.

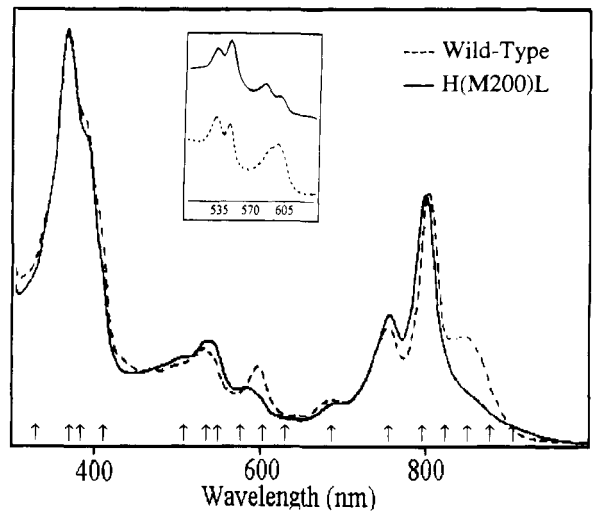

FIGURE 1: Ambient-temperature absorption spectra of wild-type and H(M200)L mutant *Rb. capsulatus* RCs. (Inset) Expanded view of the low-temperature (77 K) absorption spectrum in the Q_x region. The arrows indicate the different excitation wavelengths used to acquire RR spectra.

MATERIALS AND METHODS

The wild-type and H(M200)L mutant RCs from *Rb. capsulatus* were prepared and purified as described by Bylina and Youvan (1987, 1988). The Q_A^- RCs were prepared by adding a slight excess of sodium dithionite or ascorbic acid under illumination. The P^+ RCs from wild-type were prepared by adding a small amount of potassium ferricyanide. The D^+ RCs from the H(M200)L mutant were prepared by adding a small amount of the oxidation mediator potassium tetracyanomono(1,10-phenanthroline)ferrate(III) tetrahydrate (Schilt, 1960) as described by Nagarajan et al. (1993).

The RR spectra were obtained using methods and instrumentation previously described (Palaniappan et al., 1993). A typical data acquisition protocol consisted of coaddition of two to four 1-h (30 × 120 s) scans. All spectra were recorded at 200 K. The laser powers were typically 2 mW or less. The spectral resolution was ~2 cm^{-1} at a Raman shift of 1600 cm^{-1}. The spectral data were calibrated using the known frequencies of indene.

RESULTS

The ambient-temperature absorption spectra of the H(M200)L mutant and wild-type RCs are compared in Figure 1. An expanded view of the low-temperature (77 K) absorption spectrum in the Q_x region is shown in the inset. The spectral differences between the mutant and wild-type RCs are more clearly seen in the low-temperature spectrum due to the sharpening of the features. The various exciting lines used to probe the Q_A^- RCs are indicated by the arrows in the figure. The RR spectra of the P^+ and D^+ RCs were

obtained at a selected number of these excitation wavelengths. The choice of exciting lines for the studies of both the Q_A^- and P^+/D^+ RCs was governed by several factors. The foremost objective was to probe the different bacteriochlorin cofactors in the H(M200)L mutant RCs with as much selectivity as possible. These studies were guided in part by our earlier studies on this mutant (Peloquin et al., 1990b) and by the results of our detailed RR study of *Rb. sphaeroides* wild-type RCs wherein the high-frequency ring-skeletal and carbonyl modes of all six bacteriochlorin cofactors were assigned (Palaniappan et al., 1993). Our previous studies of *Rb. capsulatus* RCs, along with the work reported herein, indicate that the vibrational characteristics of the bacteriochlorins in wild-type RCs from *Rb. capsulatus* and *Rb. sphaeroides* are similar (Peloquin et al., 1990a,b; Palaniappan & Bocian, 1992; Palaniappan et al., 1993). Consequently, the vibrational assignments available for the cofactors in the latter RCs serve as the benchmark for the interpretation of the RR spectra of the RCs from *Rb. capsulatus*.

The RR studies of the H(M200)L mutant RCs were also guided by the desire to characterize the absorption features which distinguish the mutant from the wild-type (Bylina & Youvan, 1988; Breton et al., 1989). Inspection of Figure 1 reveals that the spectra of the two types of RCs are different in number of respects. The most significant difference is observed in the Q_y band of the primary donor (825−900 nm). The red band of D is much weaker than that of P and may consist of two separate features (DiMagno et al., 1990; Hammes et al., 1990). The Q_y bands of the accessory BChs (~800 nm) of the H(M200)L mutant RCs also appear to be slightly blue-shifted relative to those of wild-type. In the Q_x region (530−620 nm), the absorption spectrum of the mutant is more complicated than that of wild-type. In wild-type RCs, the Q_x bands of P and the two accessory BChs are overlapped and lie on the red and blue sides, respectively, of the 600-nm absorption feature; the Q_x bands of BPh_L and BPh_M occur at 545 and 530 nm, respectively (Rafferty & Clayton, 1979a,b; Kirmaier et al., 1985). The H(M200)L mutant RCs exhibit decreased absorption on the red side of the 600-nm band, a new feature at 580 nm, and increased absorption at 550 nm. The origin of the 580- and 550-nm bands is not entirely certain although Breton et al. (1989) have suggested that the former is due to a structurally perturbed accessory BCh whereas the latter is associated with D. It is not clear whether D also contributes to the absorption band at 600 nm. In the B-absorption region (350−400 nm), more subtle spectral differences are observed between the H(M200)L mutant and wild-type RCs. It is difficult to associate these changes with a particular bacteriochlorin cofactor because the B bands of all six cofactors overlap.

The specific features observed in the RR spectra of the RCs with excitation in the different absorption regions are described in detail below. In presenting the RR results, we focus exclusively on spectral data which point out structural and/or electronic differences in a particular bacteriochlorin cofactor of the H(M200)L mutant versus wild-type RCs. The RR data indicate that these differences are confined to the primary donor and the accessory BChs. The BPhs are not affected by heterodimer formation (Peloquin et al., 1990b). Accordingly, the spectral characteristics of these latter cofactors will not be discussed. We first describe the RR spectra of the Q_A^- RCs. We then proceed to the changes

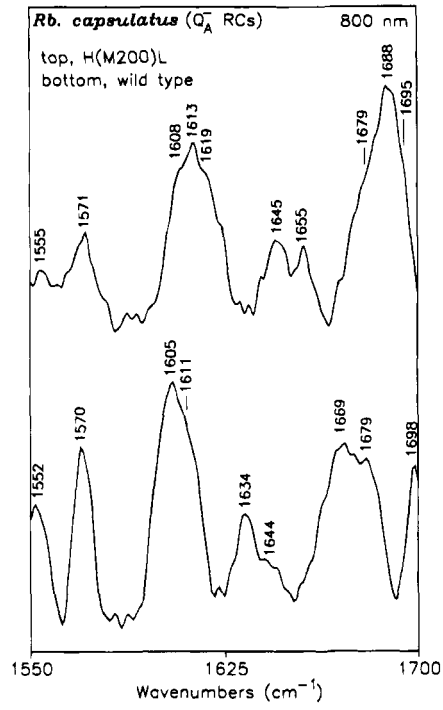

FIGURE 2: High-frequency regions of the Q_y-excitation (λ_{ex} = 800 nm) RR spectra of wild-type and H(M200)L mutant RCs.

that occur in the RR spectra upon oxidation of the primary donor.

Q_A^- RCs. (1) Q_y-Excitation RR Spectra. RR spectra of the H(M200)L mutant and wild-type RCs were obtained at a number of excitation wavelengths which span the Q_y absorptions of the different bacteriochlorin cofactors (680−900 nm). The main objective of these studies was to obtain spectra with excitation into the lowest energy absorption band(s) of D. Toward this end, attempts were made to acquire data at several different excitation wavelengths (λ_{ex} = 825−900 nm) within the contour of this band. In all cases, data acquisition conditions that resulted in reasonable quality spectra for wild-type RCs yielded extremely poor quality spectra for the mutant (not shown). The signal-to-noise ratios in these spectra are so low that it is not possible to draw any conclusions regarding the RR signatures of D. The poor quality spectra cannot be attributed to factors such as interference from fluorescence because the background emission is comparable in the H(M200)L mutant and wild-type RCs. Instead, the intrinsic RR scattering from D appears to be less than that from P, probably due in part to fact that the red absorption band of D is relatively broad and weak (Figure 1).

Representative high-frequency (1550−1700 cm^{-1}) RR spectra of the H(M200)L mutant and wild-type RCs obtained with λ_{ex} = 800 nm are shown in Figure 2. This excitation wavelength is resonant with the Q_y bands of the accessory BChs. Although the signal-to-noise ratios are relatively modest, certain differences are apparent in the band frequencies and relative intensities of the mutant versus wild-type RCs. For example, the band envelope in the 1615−1620-cm^{-1} region is shifted to higher frequency in the mutant. These bands are due to ring-skeletal vibrations of the macrocycle including the ν_{10}-like modes (Lutz, 1984; Callahan & Cotton, 1987; Palaniappan et al., 1993; Diers & Bocian, 1994). Spectral differences are also observed in the region of the νC_{2a}=O and νC_9=O which occur in the 1660−

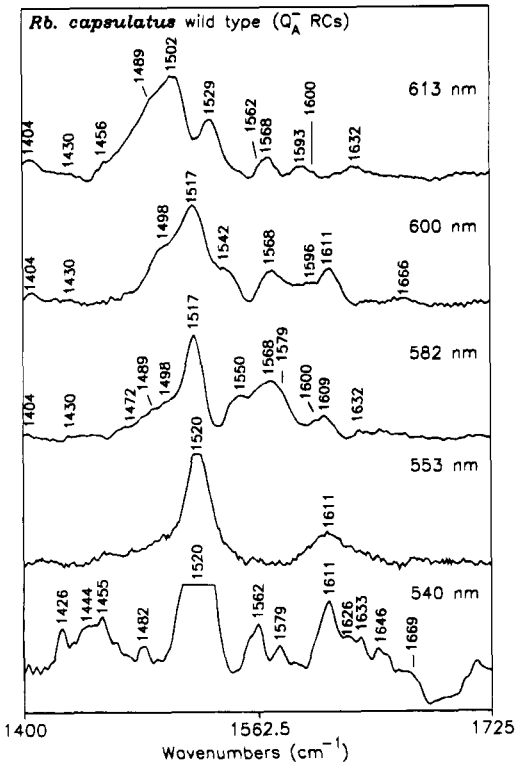

FIGURE 3: High-frequency regions of the Q_x-excitation (λ_{ex} = 540, 553, 582, 600, and 613 nm) RR spectra of quinone-reduced (Q_A^-) wild-type RCs.

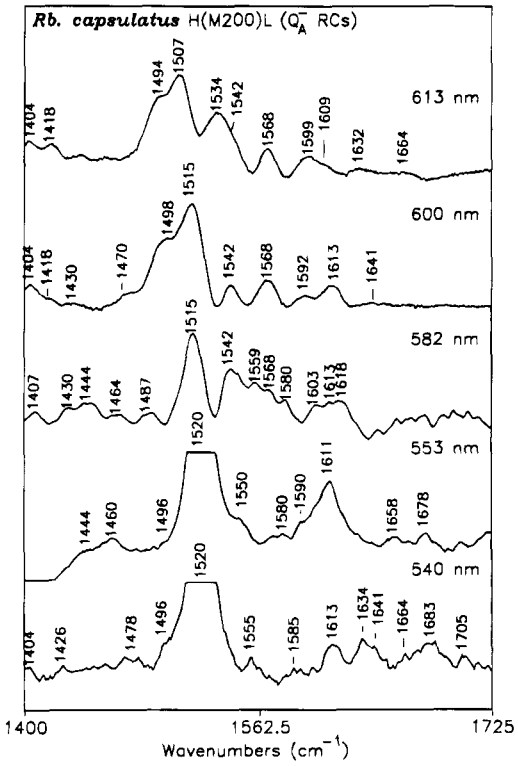

FIGURE 4: High-frequency regions of the Q_x-excitation (λ_{ex} = 540, 553, 582, 600, and 613 nm) RR spectra quinone-reduced (Q_A^-) H(M200)L mutant RCs.

1700-cm^{-1} region (Lutz & Robert, 1988; Robert, 1990; Lutz & Mäntele, 1991; Palaniappan & Bocian, 1992; Palaniappan et al., 1993). Collectively, the Q_y-excitation RR data suggest that the scattering characteristics of the accessory BChs in H(M200)L mutant RCs are different from those in wild-type RCs. The view is confirmed by the RR data obtained with B and Q_x excitation (vide infra).

(2) Q_x-Excitation RR Spectra. RR spectra of the H(M200)L mutant and wild-type RCs were obtained at a number of excitation wavelengths which span the Q_x absorptions of the different bacteriochlorin cofactors (500−615 nm). Representative high-frequency (1400−1725 cm^{-1}) RR spectra acquired with λ_{ex} = 613, 600, 582, 553, and 540 nm are shown in Figures 3 and 4, respectively. These spectra are presented for the following reasons: In wild-type RCs, λ_{ex} = 613 nm results in scattering exclusively from P (Palaniappan et al., 1993). With λ_{ex} = 600 nm, both P and the accessory BChs scatter; however, the RR spectrum is dominated by contributions from the latter cofactors. Accordingly, RR spectra obtained for the H(M200)L mutant RCs at these two excitation wavelengths should provide information on whether D contributes to the 600-nm absorption band of the mutant. Similarly, the RR data obtained for the mutant with λ_{ex} = 582 and 553 nm should provide information concerning the identity of cofactors responsible for these new absorption bands. The RR spectra acquired with λ_{ex} = 540 nm are shown to provide contrast with those obtained with λ_{ex} = 553 nm. The former exciting line falls between the Q_x bands of BPh_L and BPh_M (vide supra).

With λ_{ex} = 613 nm, strong RR scattering is observed for the H(M200)L mutant RCs (Figure 4, top trace). Bands assignable to ring-skeletal vibrations of a BCh are observed at 1494, 1507, 1534, 1568, 1599, and 1609 cm^{-1} (Palaniappan et al., 1993; Diers & Bocian, 1994) . Upon shifting to λ_{ex} = 600 nm, the general appearance of the RR spectrum changes and bands are observed at 1498, 1515, 1542, 1568, 1592, and 1613 cm^{-1} (Figure 4, second trace). All of these bands are also assignable to ring-skeletal fundamentals of a BCh although a carotenoid band centered near 1520 cm^{-1} most likely also contributes to the band envelope in the 1515−1525 cm^{-1} region (Koyama et al., 1982, 1983; Lutz, 1984; Lutz et al., 1988; Robert, 1990). The fact that the RR spectrum of the H(M200)L mutant RCs changes as the excitation wavelength is shifted from 613 to 600 nm parallels the behavior observed for wild-type (cf. Figure 3, top and second traces). The results obtained for the mutant indicate that, as is the case for wild-type, different cofactors with different absorption characteristics are contributing to the RR spectra at the two excitation wavelengths. The most consistent explanation for the full body of data, including that obtained for the D^+ RCs (vide infra), is that the BCh in D [D_L(BCh)] is responsible for the spectrum observed with λ_{ex} = 613 nm. Accordingly, the Q_x band of this cofactor lies on the red side of the 600-nm absorption band. For both the mutant and wild-type RCs, the RR spectrum observed with λ_{ex} = 600 nm is due to the accessory BChs.

Comparison of the RR spectra of the H(M200)L mutant and wild-type RCs acquired with λ_{ex} = 613 and 600 nm reveals certain other noteworthy features:

(1) With λ_{ex} = 613 nm (resonant with the primary donor), the RR spectra of the mutant and wild-type RCs are different. In particular, the bands due to certain ring-skeletal vibrations of the mutant are upshifted relative to those of the wild-type. For example, the mutant exhibits bands at 1494, 1507, and 1534 cm^{-1}; the analogous bands in wild-type occur at 1489, 1502, and 1529 cm^{-1}. This observation suggests that the skeletal-mode frequencies of D_L(BCh) are intrinsically different from those of either P_L or P_M, consistent with the

results of FT-IR studies of the heterodimer mutants (Nabedryk et al., 1992). It should be noted, however, that the RR spectrum of wild-type RCs is a composite spectrum due to the overlapped bands of both P_L and P_M and that the skeletal-mode frequencies of these two cofactors are different (Palaniappan et al., 1993). The frequencies of one of the BChs in P are similar to those of the accessory BChs; the frequencies of the other BCh are lower. It is uncertain which set of modes is associated with which BCh in P. Comparison of the frequencies of the RR bands of D_L(BCh) with those of the composite bands due to P_L and P_M suggests that the bands of D_L(BCh) are closer to those of the BCh in P which exhibits the higher set of skeletal-mode frequencies. For example, D_L(BCh) exhibits bands at 1568, 1508, and 1494 cm^{-1}; the pairs of bands for P are observed at 1568/1561, 1508/1500, and 1494/1488 cm^{-1} (Palaniappan et al., 1993). The most straightforward explanation for this result is that the skeletal-mode frequencies of D_L(BCh) are more similar to those of P_L than P_M. Accordingly, P_M of wild-type RCs exhibits anomalously low skeletal-mode frequencies.

(2) With $\lambda_{ex} = 600$ nm (resonant with the accessory BChs), the frequencies observed for the RR bands of the H(M200)L mutant and wild-type RCs are very similar to one another. [In the latter RCs, the frequencies of the ring-skeletal modes of BCh_L and BCh_M are nearly identical (within the RR line width), and the bands observed with $\lambda_{ex} = 600$ nm are due to the overlap of these unresolved features (Palaniappan et al., 1993).] This result is seemingly inconsistent with Q_y-excitation spectra in which the ν_{10}-like band envelope of the accessory BChs of the H(M200)L mutant RCs is distinctly upshifted from that of wild-type (Figure 2). The apparent inconsistency is partially resolved by closer inspection of the RR data obtained with $\lambda_{ex} = 600$ nm. At this excitation wavelength, the RR bands of the mutant are sharper and better resolved than those of the wild type (cf. Figures 3 and 4, second traces). The sharper features observed for the mutant can be explained if only one of the two accessory BChs contributes strongly to the spectrum acquired with $\lambda_{ex} = 600$ nm. This interpretation is further consistent with the features observed in the spectra acquired with $\lambda_{ex} = 582$ nm (vide infra).

With $\lambda_{ex} = 582$ nm, the RR spectrum of the H(M200)L mutant RCs is different from that of wild-type (cf. Figures 3 and 4, third traces). In particular, the mutant exhibits many more bands assignable to ring-skeletal vibrations of a BCh (Palaniappan et al., 1993; Diers & Bocian, 1994). It is reasonable to assume that these modes gain resonance enhancement via excitation of the 580-nm absorption band. It is difficult to identify all of the new RR bands because these features overlap with bands which are enhanced via the 600-nm absorption. (Note that significant RR scattering is also observed for wild-type RCs with $\lambda_{ex} = 582$ nm.) Nevertheless, one particularly noteworthy feature of the RR spectra acquired with $\lambda_{ex} = 582$ nm is that a band is observed for the mutant near 1618 cm^{-1} which is absent in the wild-type. The highest frequency band of appreciable intensity for the latter RCs is the ν_{10}-like mode near 1609 cm^{-1}. Similarly, the ν_{10}-like bands near 1611−1613 cm^{-1} are also the highest frequency modes observed for both the mutant and wild-type RCs with $\lambda_{ex} = 600$ nm (cf. Figures 3 and 4, second traces). The most consistent explanation for all these data is that the 1618-cm^{-1} band observed with $\lambda_{ex} = 582$ nm is due to a ν_{10}-like mode of a structurally perturbed accessory BCh and that the 580 nm absorption is the Q_x band of this cofactor. This interpretation resolves the apparent inconsistency in the RR spectra of the mutant observed with $\lambda_{ex} = 600$ versus 800 nm. In particular, the normal versus upshifted ν_{10}-like band envelopes are due to the contribution of only one of the two accessory BChs to the former spectrum and both to the latter. This in turn implies that the Q_y absorptions of the two accessory BChs in the mutant are at approximately the same energy, which is consistent with the general appearance of the optical spectrum (Figure 1).

With $\lambda_{ex} = 553$ nm, the RR spectra of the H(M200)L mutant and wild-type RCs are also different from one another (cf. Figures 3 and 4, fourth traces). In the case of the wild-type, the only discernible features are the carotenoid band at 1520 cm^{-1} and a broad, unresolved contour which maximizes near 1611 cm^{-1}. This latter feature is probably be due to preresonant scattering from BPh_L and BPh_M. In the spectrum of the mutant, many more distinct features are observed including bands at 1550, 1580, 1590, 1611, 1658, and 1678 cm^{-1}. The appearance of these distinct features is attributed to resonant scattering via the 550-nm absorption band of the mutant. The four lower frequency bands are assignable to ring-skeletal fundamentals of a BPh molecule (Palaniappan et al., 1993; Diers & Bocian, 1994). The 1658- and 1678-cm^{-1} bands are assignable to the νC_{2a}=O, and νC_9=O vibrations, respectively (Lutz & Robert, 1988; Robert, 1990; Lutz & Mäntele, 1991; Palaniappan et al., 1993). Collectively, the RR scattering characteristics observed for the mutant with $\lambda_{ex} = 553$ nm are best explained if the BPh in D [D_M(BPh)] is the principal contributor to the spectrum and the 550-nm absorption is the Q_x band of this cofactor. The RR data obtained for D_M(BPh) are the first which unambiguously reveal the ring-skeletal and carbonyl frequencies for the BPh cofactor in heterodimer mutants.

(3) B-Excitation RR Spectra. RR spectra of the H(M200)L and wild-type RCs were obtained at several excitation wavelengths within the B absorption bands of the various pigments. The spectra of the mutant and wild-type are similar with $\lambda_{ex} = 407$ nm and also with 364 nm (not shown), consistent with previous observations (Peloquin et al., 1990b). In wild-type RCs, excitation on the red side of the B band contour results in RR scattering predominantly from the two accessory BChs whereas excitation near the maximum results in scattering predominantly from the two BPhs. There is very little contribution to the RR spectra from P with either $\lambda_{ex} = 407$ or 364 nm (Lutz, 1984; Lutz & Robert, 1988). The similarity in the RR spectra of the mutant and wild-type obtained with $\lambda_{ex} = 364$ nm is consistent with the full body of RR data which indicates that the BPhs are not affected by heterodimer formation. On the other hand, the fact that the RR spectra of the mutant and wild-type RCs are similar with $\lambda_{ex} = 407$ nm suggests that only the "normal" accessory BCh ($Q_x \sim 600$ nm) strongly contribute to the spectrum of the mutant. This in turn implies that the B absorptions of the perturbed accessory BCh ($Q_x \sim 580$ nm) are shifted to higher energy. Therefore, the RR investigations were extended to bluer excitation wavelengths.

The high-frequency (1400−1725 cm^{-1}) RR spectra of the H(M200)L mutant and wild-type RCs obtained with $\lambda_{ex} =$ 356 nm are compared in Figure 5. At this excitation wavelength, the RR spectra of the mutant and wild-type RCs

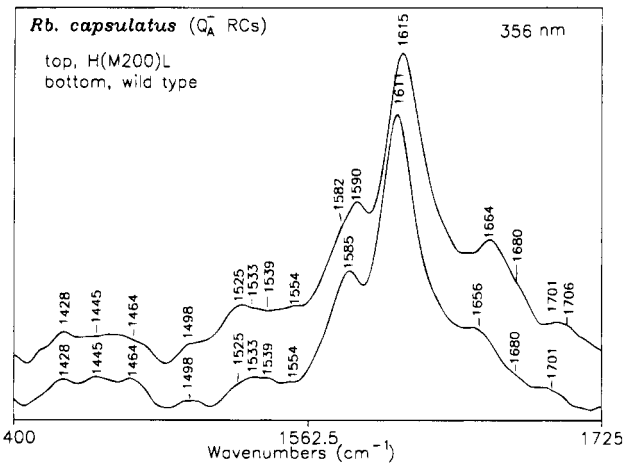

FIGURE 5: High-frequency regions of the B-excitation (λ_{ex} = 356 nm) RR spectra of quinone-reduced (Q_A^-) wild-type and H(M200)L mutant RCs.

are different from each other, unlike the spectra obtained with λ_{ex} = 407 nm. The most notable difference is that the ν_{10}-like band envelope is upshifted by ~4 cm^{-1} in the mutant (1615 cm^{-1}) versus wild-type (1611 cm^{-1}) RCs. The ν_{10}-like profile of the mutant is also much broader than that of wild-type [~40% (FWHM)]. Other differences are also clearly visible in the RR spectra of the mutant versus wild-type RCs. For example, a new RR band is observed for the mutant at ~1590 cm^{-1}. The observation that the ν_{10}-like band envelope of the mutant is broadened and upshifted suggests that the perturbed accessory BCh is primarily responsible for the altered RR spectrum seen with λ_{ex} = 356 nm. This type of spectral signature would not occur if either D_L(BCh) or D_M(BPh) were the principal contributors because the ν_{10}-like bands of these cofactors are both in the 1609–1611-cm^{-1} range (Figure 4, top and fourth traces).

D^+ and P^+ RCs. (1) Q_x-Excitation RR Spectra. The Q_x-excitation RR spectra of chemically oxidized wild-type and H(M200)L mutant RCs are shown in Figures 6 and 7, respectively. These spectra focus on the absorption region associated with the primary donor and the accessory BChs. Comparison of the RR data obtained for the D^+/P^+ and Q_A^- RCs shows that oxidation of the primary donor results in a number of spectral changes. At certain excitation wavelengths, the oxidation-induced spectral changes are similar for the mutant and wild-type RCs, whereas at others the changes are different.

The most notable effect of oxidation on the H(M200)L mutant RCs is the complete bleaching of the RR spectrum observed with λ_{ex} = 613 nm. This behavior parallels that observed for wild-type RCs (cf. Figures 6 and 7, top traces). The oxidation-induced bleaching of the RR spectrum of the mutant unambiguously demonstrates that D contributes to the red side of the 600-nm absorption band even though this contribution is difficult to quantify based on the appearance of the spectrum in this region [Figure 1; see also Breton et al. (1989)]. The bleaching observed with λ_{ex} = 613 nm in conjunction with the nature of the oxidation-induced spectral changes observed with λ_{ex} = 553 nm (vide infra) are only consistently explained if the RR spectra observed at these two excitation wavelengths are due to D_L(BCh) and D_M-(BPh), respectively. The oxidation-induced bleaching of the RR features assigned to D_L(BCh) is consistent with the results of other spectroscopic studies of the H(M200)L mutant RCs

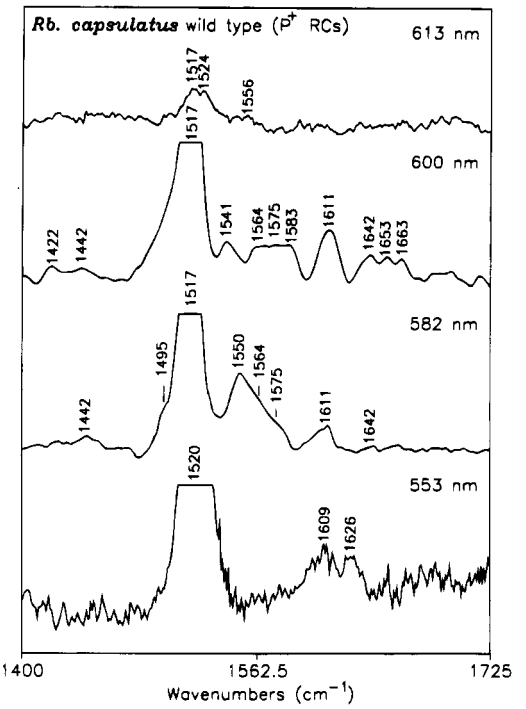

FIGURE 6: High-frequency regions of the Q_x-excitation (λ_{ex} = 553, 582, 600, and 613 nm) RR spectra of oxidized (P^+) wild-type RCs.

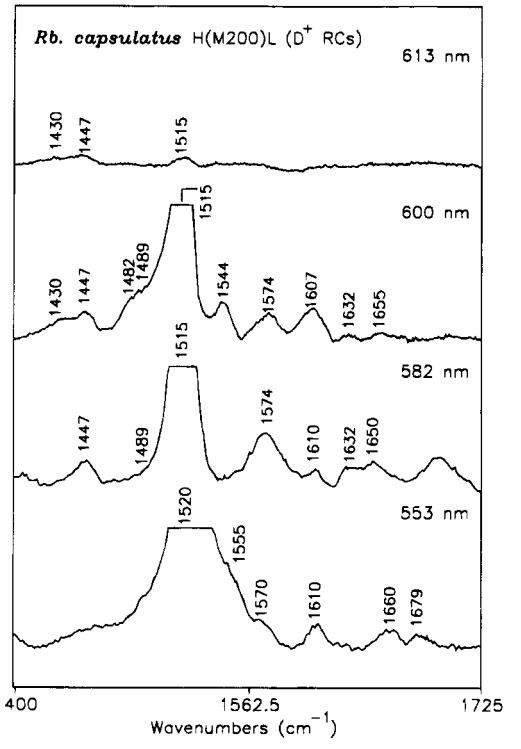

FIGURE 7: High-frequency regions of the Q_x-excitation (λ_{ex} = 553, 582, 600, and 613 nm) RR spectra of oxidized (D^+) H(M200)L mutant RCs.

which indicate that the hole of D^+ is localized on this cofactor (Bylina et al., 1990; Huber et al., 1990; Nabedryk et al., 1992).

Oxidation also affects the general appearance of the RR spectra of the accessory BChs of the H(M200)L mutant RCs obtained with λ_{ex} = 600 and 582 nm. These perturbations include band shifts and intensity changes. [It should be emphasized that neither the 600- nor 580-nm absorption bands of the mutant bleach upon D^+ formation (Breton et

al., 1989).] The fact that formation of D^+ affects the RR spectra of the accessory BChs in the mutant RCs parallels the behavior observed upon P^+ formation in wild-type (cf. Figures 6 and 7, second and third traces; Palaniappan & Bocian, 1992; Palaniappan et al., 1993). However, closer inspection of the RR spectra of the mutant and wild-type RCs obtained with λ_{ex} = 600 and 582 nm shows that the oxidation-induced changes in the scattering characteristics of the accessory BChs are not the same for the two RCs. These differences may reflect the fact that the charge distribution is not the same in D^+ versus P^+ RCs (Bylina et al., 1990; Huber et al., 1990; Nabedryk et al., 1992; Rautter et al., 1994).

The effects of oxidation are more pronounced in the RR spectrum acquired with λ_{ex} = 553 nm than those observed with either λ_{ex} = 600 or 582 nm. In particular, formation of D^+ significantly diminishes the overall RR intensity, which is qualitatively consistent with the report that oxidation bleaches the 550-nm absorption band of the mutant (Breton et al., 1989). However, closer inspection of the RR data of the D^+ RCs shows that bands due to the ν_{10}-like mode, νC_{2a}=O, and νC_9=O are still clearly observed near 1610, 1660, and 1679 cm^{-1}, respectively. These frequencies are identical to those observed for the Q_A^- RCs (cf. Figures 4 and 7, fourth traces). These bands cannot be attributed to residual unoxidized RCs because their relative intensities are different in the spectra of D^+ and Q_A^- RCs. In the case of D^+ RCs, the ν_{10}-like mode, νC_{2a}=O, and νC_9=O are all of comparable intensity, whereas for Q_A^- RCs the ν_{10}-like mode is much stronger than either νC_{2a}=O or νC_9=O. The oxidation-induced loss of overall RR intensity along with the changes in relative RR intensities can be explained if the absorption band of the cofactor giving rise to the RR scattering is shifted, rather than bleached, upon formation of D^+. This type of behavior is consistent with D_M(BPh) being the principal contributor to the spectrum. In particular, D_M(BPh) should retain the electronic and vibrational properties of a neutral BPh in the D^+ RCs because the hole density is confined to D_L(BCh) (Bylina et al., 1990; Huber et al., 1990; Nabedryk et al., 1992). On the other hand, the energy of the Q_x absorption of D_M(BPh) might be expected to shift due to the close proximity of this cofactor to $D_L(BCh)^+$. The wavelength of the Q_x absorption band of D_M(BPh) in the D^+ RCs is not clear. [A red-shifted feature should be detectable because this region of the absorption spectrum is relatively free from other bands (Figure 1). In contrast, a blue-shifted band would be extremely difficult to detect due to interference from the Q_x bands of the BPhs and/or the carotenoid absorptions.]

(2) B Excitation RR Spectra. The B excitation spectra of the H(M200)L mutant and wild-type RCs observed with λ_{ex} = 356 nm are shown in Figure 8. As is the case for the Q_A^- RCs (Figure 5), the spectra of the D^+ and P^+ RCs are different from one another. In addition, D^+ formation much more strongly perturbs the appearance of the RR spectrum than does P^+ formation. The spectral changes observed for the H(M200)L mutant RCs include frequency shifts, the appearance of new bands (for example, 1580 cm^{-1}), and a considerable filling in of the envelope of RR bands in the 1500−1650-cm^{-1} region. This latter observation suggests that many new, unresolved bands are contributing to the RR spectrum of the D^+ RCs in this region. In contrast, the P^+ formation appears to sharpen the spectral features as opposed to broaden them.

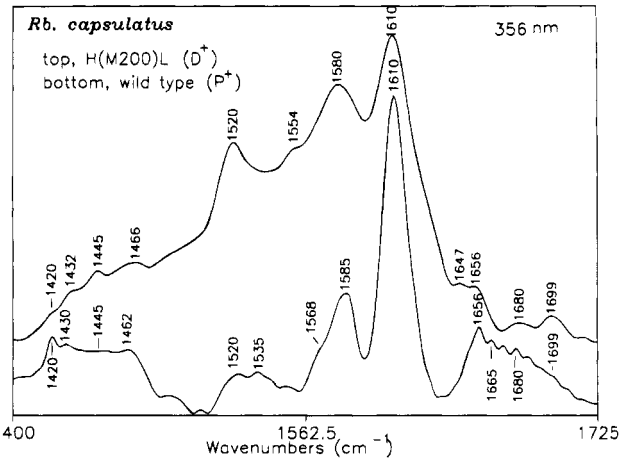

FIGURE 8: High-frequency regions of the B-excitation (λ_{ex} = 356 nm) RR spectra of oxidized wild-type (P^+) and H(M200)L mutant (D^+) RCs.

The fact that all six pigments in the RC contribute to the B absorption band precludes a detailed interpretation of the oxidation-induced changes observed in the RR spectrum of the H(M200)L mutant RCs. Nevertheless, the dramatic differences observed in the spectra of D^+ versus P^+ RCs strongly suggest that the primary donor must be involved. The RR data obtained at other excitation wavelengths do not provide any information on the scattering characteristics of $D_L(BCh)^+$ versus P^+. However, the fact that the hole in oxidized H(M200)L mutant RCs is localized on $D_L(BCh)^+$ suggests that the RR features of this cation radical should be similar to those of monomeric BCh^+. Indeed, comparison of the spectra of the D^+ RCs with those of five-coordinate BCh^+ reveals many features in common (Diers & Bocian, 1994). For example, the ν_{10}-like band of BCh^+ is downshifted from that of the neutral by ~5 cm^{-1}. In addition, with λ_{ex} = 356 nm, the 1581-cm^{-1} ring-skeletal mode is much more strongly resonance enhanced in BCh^+ than in the neutral. These comparisons suggest that $D_L(BCh)^+$ makes a significant contribution to the RR spectrum of the D^+ RCs observed with λ_{ex} = 356 nm.

(3) Carotenoid RR Scattering. As was previously noted, the carotenoid in the RCs contributes to the RR spectra acquired at a number of excitation wavelengths, particularly those in the yellow-green region (Figures 3, 4, 6, and 7). Comparison of the RR spectra of the P^+ or D^+ RCs (Figures 6 and 7) with those of the Q_A^- species (Figures 3 and 4) reveals that oxidation of the primary donor significantly increases the RR scattering intensity from the carotenoid in both the H(M200)L mutant and wild-type types of RCs. The increase in RR intensity occurs in the absence of any apparent changes in the absorption profile of the carotenoid or in its vibrational frequencies. Although the magnitude of the oxidation-induced increase in carotenoid RR scattering has not yet been quantitated, preliminary estimates indicate that the increase ranges from 2−4 depending on the excitation wavelength. These estimates were obtained by using either the intensity of the bacteriochlorin RR bands or the number of counts detected for the 1520-cm^{-1} carotenoid band as qualitative intensity standards.

DISCUSSION

The RR data obtained for the H(M200)L mutant RCs provide a much clearer picture of the effects of heterodimer

formation on the structural and electronic properties of the cofactors. These features also help resolve certain ambiguities which have arisen in the characterization of the primary donor in wild-type RCs (Palaniappan et al., 1993). In general, the RR data indicate that heterodimer formation influences not only the properties of the primary donor but also those of one of the accessory BChs. In contrast, the BPhs in the RC are not affected. We first discuss the structural and electronic properties of the heterodimer primary donor in the H(M200)L mutant RCs and their relationship to those of the homodimer in the wild-type. We then discuss the effects of heterodimer formation on the properties of the accessory BChs. Finally, we comment on the oxidation-induced perturbations on the RR scattering characteristics of the carotenoid in the *Rb. capsulatus* RCs.

Structural and Electronic Properties of the Primary Donor. The vibrational characteristics of D_L(BCh) in the H(M200)L mutant RCs indicate that the structure of this cofactor is different from that of either P_L or P_M, consistent with the results of FT-IR studies (Nabedryk et al., 1992). Nevertheless, the structure of D_L(BCh) is more similar to that of one of the two BChs of P than the other. This latter cofactor is most likely P_L. These observations indicate that while substitution of BPh for BCh on the M side of the primary donor affects the structure of the BCh on the L side, the structural change is not exceptionally large. This line of logic also establishes the identity of P_L and P_M in the RR spectra of wild-type RCs. As was previously noted, earlier RR studies on the wild-type have shown that the structures of one of these cofactors is similar to those of the two accessory BChs whereas the structure of the other member of P is different (Palaniappan et al., 1993). This latter BCh is regarded as structurally unusual because the vibrational characteristics of the other three BChs are similar to those of five-coordinate BCh in solution (Callahan & Cotton, 1987; Diers & Bocian, 1994). The RR data reported herein for the H(M200)L mutant RCs indicate that P_M is the structurally unique BCh in the primary donor of wild-type RCs. The fact that the ring-skeletal frequencies of P_M are unusually low suggests that the macrocycle of this cofactor is more conformationally distorted that those of the other BChs in the RC.

The vibrational characteristics of the D_M(BPh) cofactor in the H(M200)L mutant RCs indicate that the structure of this BPh is generally similar to that of the other two BPhs in the RCs. [The structures of BPh_L and BPh_M are not exactly identical; however, the differences are confined to the ring V region of the macrocycle (Peloquin et al., 1991; Palaniappan et al., 1993).] The structures of all the BPhs in the mutant and wild-type RCs are also similar to those of BPh in solution (Diers & Bocian, 1994). Together, these observations indicate that the protein environment on the M side of the primary donor is not sufficiently constraining to induce conformational distortions in the bacteriochlorin macrocycle. The question then remains as to why the conformation of the P_M cofactor of wild-type RCs is different from that of P_L. The most likely explanation is that P_M is distorted via the covalent bond which links the Mg(II) ion of this cofactor and the H(M200) protein residue. This linkage could affect the ring conformation either directly, by doming the macrocycle, or indirectly, by forcing P_M to reside in a location where its interactions with the protein matrix are much stronger.

The vibrational characteristics of the carbonyl stretching vibrations of D_M(BPh) in the H(M200)L mutant RCs provide additional insight into the nature of the protein environment on the M side of the primary donor. The νC_{2a}=O and νC_9=O vibrations of D_M(BPh) are observed at 1658 and 1678 cm^{-1}, respectively, close to those observed for the analogous modes of P_M in wild-type RCs (Lutz & Robert, 1988; Robert, 1990; Lutz & Mäntele, 1991; Nabedryk et al., 1992; Palaniappan et al., 1993; Mattioli et al., 1991, 1994). The νC_{2a}=O frequencies of both D_M(BPh) and P_M are in the range expected for a non-hydrogen bonded keto group (Lutz, 1984; Lutz & Robert, 1988; Lutz & Mäntele, 1991) consistent with the fact that no residues capable of hydrogen bonding are in the vicinity of the C_{2a}-acetyl group of the M-side cofactor (Deisenhofer et al., 1985; Chang et al., 1986; Allen et al., 1986; Yeates et al., 1988; Deisenhofer & Michel, 1989b; El-Kabbani et al., 1991; Ermler et al., 1994; Chirino et al., 1994). In contrast, the νC_9=O frequencies of both D_M(BPh) and P_M are lower than those expected for a free keto group and close to those observed for hydrogen-bonded carbonyls (Lutz, 1984; Lutz & Robert, 1988; Robert, 1990; Lutz & Mäntele, 1991). Yet no protein residues capable of hydrogen bonding are in the vicinity of this group (Deisenhofer et al., 1985; Chang et al., 1986; Allen et al., 1986; Yeates et al., 1988; Deisenhofer & Michel, 1989b; El-Kabbani et al., 1991; Ermler et al., 1994; Chirino et al., 1994). Accordingly, other characteristics of the protein environment, such as the effective dielectric constant (ϵ_{eff}), must be responsible for the anomalously low νC_9=O frequencies of D_M(BPh) and P_M (Nabedryk et al., 1992; Palaniappan et al., 1993). Furthermore, this environmental perturbation appears to be specific to the M side because the frequencies of the νC_9=O vibrations of neither D_L(BCh) nor P_L are not anomalously low (Lutz & Robert, 1988; Robert, 1990; Lutz & Mäntele, 1991; Nabedryk et al., 1992; Palaniappan et al., 1993; Mattioli et al., 1991, 1994). The lower frequencies observed for the νC_9=O modes of the M-side cofactors imply that ϵ_{eff} in the region of the C_9-keto groups of P_M/D_M(BPh) is higher than that near the analogous groups of P_L/D_L(BCh) (Koyama et al., 1986; Krawczyk, 1989). At this time, no additional data are available concerning ϵ_{eff}(M) versus ϵ_{eff}-(L) in the vicinity of the primary donor. However, Steffan et al. (1994) concluded from Stark effect measurements on the BPhs and accessory BChs that a significant dielectric asymmetry exists in wild-type RCs and that ϵ_{eff}(L) > ϵ_{eff}-(M). Palaniappan and Bocian (1995) have shown that the magnitude and direction of the asymmetry predicted by the Stark effect measurements provides a self-consistent explanation for the frequency differences observed for the νC_9=O modes of BPh_L versus BPh_M in E(L104)L mutant RCs. Taken together with our present results, these studies suggest that the L- versus M-side dielectric asymmetry reverses between the primary donor and acceptor. The magnitudes and directions of these asymmetries could have a significant effect on the free energies of the various electronic states of the cofactors and hence on the electron transfer kinetics.

One final point concerns the nature of the Q_x excited states of the primary donors in both the H(M200)L mutant and wild-type RCs. As was previously noted, the Q_x bands of D_L(BCh) and D_M(BPh) occur near 600 and 550 nm, respectively. These wavelengths are near those observed for monomeric BCh and BPh, which suggests that the interac-

tions between the Q_x excited states of the cofactors in the heterodimer are relatively weak. The fact that Q_x-Q_x coupling is small is not surprising given the large intrinsic difference between the energies of the Q_x states of BCh and BPh and the relatively small magnitude of the Q_x transition dipole moments. In the case of wild-type RCs, a Q_x band of P also occurs near 600 nm (Rafferty & Clayton, 1978a,b; Kirmaier et al., 1985). However, it has never been unambiguously established whether this band is due to the Q_x bands of both P_L and P_M, which overlap due to minimal coupling between the Q_x excited states, or to one member of an exciton pair which arises from coupling of the Q_x states (Rafferty & Clayton, 1978 a,b). The fact that the Q_x bands of P and D_L(BCh) occur in the same region supports the view that the 600-nm absorption of P is due to the overlapped Q_x absorptions of both P_L and P_M. The fact that P^+ formation completely bleaches the absorption and RR spectra indicates that there is some coupling between the Q_x states of the cofactors in the homodimer. This coupling provides a mechanism to mix cation radical character into both BChs in P^+ RCs. In the absence of coupling, the spectra of P^+ would necessarily contain contributions from a neutral as well as cationic species. This behavior is not observed.

Structural and Electronic Properties of the Accessory BChs. The vibrational characteristics of the accessory BChs in the H(M200)L mutant RCs indicate that the structure of one of the two cofactors is perturbed by heterodimer formation (anomalously high frequency for the ν_{10}-like mode). The absorption characteristics of the perturbed accessory BCh in the mutant are also consistent with a structural perturbation. This is evidenced by the fact that the perturbation strongly affects the Q_x band (~20-nm blue-shift) but has minimal effect on the Q_y absorption (<5-nm blue-shift). This shift pattern is characteristic of a change in the conformation of the macrocycle (Callahan & Cotton, 1987). In contrast, a change in the electronic interaction between the accessory BCh and a neighboring cofactor might be expected to more strongly influence the Q_y bands. The ~20-nm difference observed for the Q_x bands of the two accessory BChs in the H(M200)L mutant RCs is in the range typically associated with five- versus six-coordinate BCh (Callahan & Cotton, 1987). However, the observed energy ordering for the Q_x bands could only be reconciled if the ~600- and 580-nm absorbing BChs are six- and five-coordinate, respectively. This possibility is incompatible with the five-coordinate structure known for the accessory BChs in wild-type RCs (Deisenhofer et al., 1985; Deisenhofer & Michel, 1989b; Ermler et al., 1994; Deisenhofer et al., 1995).

The question remains as to which of the two accessory BChs is perturbed by heterodimer formation. The RR data obtained for the H(M200)L mutant RCs cannot be used to identify this accessory BChs because the vibrational signatures of both accessory BChs in wild-type RCs are essentially identical (Palaniappan et al., 1993). Furthermore, it is difficult to visualize how heterodimer formation would induce a structural change in one of the accessory BChs. The primary donor and the accessory BChs are spatially separated (Deisenhofer et al., 1985, 1995; Chang et al., 1986; Allen et al., 1986; Yeates et al., 1988; Deisenhofer & Michel, 1989b; El-Kabbani et al., 1991; Ermler et al., 1994). In addition, the X-ray crystallographic data obtained for heterodimer mutant RCs from *Rb. sphaeroides* do not suggest that one of the accessory BChs occupies a position in the protein which is significantly different from that in wild-type (Chirino et al., 1994). On the other hand, the resolution of these data is not sufficient to determine whether the detailed structure of one of the accessory BChs is altered in the heterodimer RCs. Accordingly, we can only speculate as to which accessory BCh is perturbed in the H(M200)L mutant RCs. In the case of the M-side heterodimer, the most likely candidate would seem to be BCh_L. This choice is based on the fact that BCh_L is closer to the M side of the primary donor than is BCh_M (Deisenhofer et al., 1985; Chang et al., 1986; Allen et al., 1986; Yeates et al., 1988; Deisenhofer & Michel, 1989b; El-Kabbani et al., 1991; Ermler et al., 1994). In addition, the BCh_L in wild-type RCs is connected to the H(M200) residue, which serves as the axial ligand to P_M, via a water network (Deisenhofer & Michel, 1989b; Ermler et al., 1994). This interaction would be disrupted upon replacement of histidine with leucine. Regardless of the origin of the structural perturbation, the spectroscopic data indicate that this perturbation is significant. This in turn could affect the free energy and redox properties of the BCh macrocycle (Barkigia et al., 1988) and possibly the detailed features of the electron-transfer kinetics in the RC.

Primary Donor Oxidation State and Carotenoid RR Scattering. The observation that primary donor oxidation substantially increases the carotenoid RR scattering intensity in both the H(M200)L mutant and wild-type RCs from *Rb. capsulatus* is totally unexpected. No such effects were observed in our previous RR studies of wild-type RCs from *Rb. sphaeroides* (Palaniappan et al., 1993). The origin of the oxidation-induced enhancement of the carotenoid RR scattering is not certain; however, it seems highly unlikely that the effect is dependent on the particular species of bacteria from which the RCs are obtained. Instead, the effect is most likely determined by the nature of the carotenoids in the RCs. The *Rb. capsulatus* RCs were prepared under semiaerobic conditions (Bylina & Youvan, 1987, 1988), which leads to the incorporation of a mixture sphaeroidene and sphaeroidenone (Frank & Cogdell, 1993). The *Rb. sphaeroides* RCs were prepared under anaerobic conditions (McGann & Frank, 1985), which leads to the near exclusive incorporation of sphaeroidene (Cogdell et al., 1976). Sphaeroidene contains 10 C=C bonds in the conjugation pathway, whereas sphaeroidenone contains an additional conjugated C=O group. As a consequence, the principal absorption features of sphaeroidenone are red-shifted relative to those of sphaeroidene (Frank & Cogdell, 1993). The question remains as to how the RR scattering intensity of one type of carotenoid and not the other is affected by primary donor oxidation.

The RR cross section is dictated by a number of factors including the intrinsic oscillator strength of the electronic transition, the Frank−Condon overlaps, and the dephasing rates on the excited-state surface (Myers & Mathies, 1987). The oxidation-induced enhancement of RR scattering from the carotenoid in the *Rb. capsulatus* RCs is best rationalized in terms of the changes in the dephasing rates in the S_2 excited state of this chromophore. This factor is implicated because P^+/D^+ formation does not appear to alter the absorption spectrum of the carotenoid. The stronger carotenoid scattering from the P^+/D^+ RCs implies a decreased dephasing rate. The dephasing rate of the S_2 state of the

carotenoid could be affected by P^+/D^+ formation if this state is coupled to the Q_x state(s) of the primary donor. The observation that the RR cross section of sphaeroidenone is perturbed by primary donor oxidation whereas that of sphaeroidene is not implies that the S_2-Q_x coupling is stronger in the former carotenoid. This could arise because the S_2 state of sphaeroidenone energetically closer to the Q_x of the primary donor (Frank & Cogdell, 1993). It is also possible that the two carotenoids are in somewhat different locations in the protein pocket and that sphaeroidenone is closer to the primary donor.

The fact that S_2-Q_x coupling has any effect on the RR cross section of the carotenoid is remarkable. The dephasing rates in carotenoids are necessarily extremely fast considering that the $S_2 \rightarrow S_1$ internal conversion rates in these polyenes are in the 100−200 fs range (Bondarev et al., 1988; Shreve et al., 1991a,b). In order to affect the RR cross section, the time scale of the processes that mediate the S_2-Q_x coupling must be competitive with the dephasing rates (Myers & Mathies, 1987). At present, no detailed information is available on the S_2-Q_x interactions in RCs. On the other hand, these interactions have been investigated in B800−850 light-harvesting complexes (Trautman et al., 1990; Shreve et al., 1991c). These studies have shown that subpicosecond energy transfer occurs between the S_2 state of the carotenoid and the Q_x state of the BCh cofactors in the light-harvesting complex. Presuming that similar energy transfer pathways are open in RCs, the rates are apparently not fast enough to compete with the intrinsic dephasing rates that determine the RR cross section of sphaeroidene in RCs. On the other hand, the energy-transfer rate becomes competitive when sphaeroidenone is present. This implies that the energy-transfer rate is extraordinarily fast and in the range of 100 fs or less (using the $S_2 \rightarrow S_1$ internal conversion rate of the carotenoid as a benchmark). Additional static and time-resolved spectroscopic studies are clearly needed to address the issue further.

SUMMARY AND CONCLUSIONS

The RR data obtained for the H(M200)L mutant RCs indicate that heterodimer formation induces a variety of changes in the structural and electronic properties of the cofactors in the RC. These perturbations extend beyond the primary donor and include one of the two accessory BChs. In the case of the primary donor, the structure of D_L(BCh) is different from that of either P_L or P_M. This result is not particularly surprising considering the possible changes that might occur in cofactor−protein interactions upon loss of a covalent bond between the protein and half of the dimer. The vibrational characteristics of the C_9-keto carbonyl modes of both D_M(BPh) and P_M support the notion that the effective dielectric constant is different on the L- versus M-sides of the primary donor. The direction of the asymmetry appears to be opposite to that in the region of the accessory BChs and BPhs. The fact that heterodimer formation perturbs the structural and electronic properties of one of the accessory BChs is not expected nor easily rationalized in terms of the structure of the RCs. Regardless, this observation suggests that global rearrangements occur in the protein secondary structure when the ligand to a cofactor in the primary donor is removed. It is not certain to what extent these structural and electronic changes influence the kinetics of the various electron-transfer processes in the RC. However, it is clear that they are not sufficient to alter the unidirectionality of electron transfer in the H(M200)L mutant (Kirmaier et al., 1988, 1989; McDowell et al., 1990, 1991a,b; Laporte et al., 1993). Finally, the RR data obtained for both the H(M200)L mutant and wild-type RCs provide evidence for a surprisingly strong interaction between the primary donor and the carotenoid in RCs. These interactions suggest that energy transfer between these cofactors is extremely fast (100 fs or less). These processes have obvious implications for the functional behavior of carotenoids in RCs which include both singlet and triplet energy transfer (Frank & Cogdell, 1993). The fact that the RR cross section of the carotenoid is extremely sensitive to carotenoid−primary donor interactions opens new avenues for investigation of the S_2 excited-state dynamics of the carotenoid in RCs.

ACKNOWLEDGMENT

We thank Drs. E. J. Bylina, D. C. Youvan, and C. Kirmaier for providing the RCs from *Rb. capsulatus*. We also thank Drs. D. Holten, H. A. Frank, and A. P. Shreve for insightful discussions.

REFERENCES

Allen, J. P., Feher, G., Yeates, T. O., Rees, D. C., Deisenhofer, J., Michel, H., & Huber, R. (1986) *Proc. Natl. Acad. Sci. U.S.A. 83*, 8589−8593.

Barkigia, K. M., Chantranupong, L., Smith, K. M., & Fajer, J. (1988) *J. Am. Chem. Soc. 110*, 7566−7567.

Bondarev, S. L., Dvornikov, S. S., & Bachilo, S. M. (1988) *Opt. Spectrosc. (USSR) 64*, 268−270.

Boxer, S. G., Goldstein, R. A., Lockhart ,D. J., Middendorf, R. T., & Takiff, L. (1989) *J. Phys. Chem. 93*, 8280−8294.

Breton, J., & Verméglio, A. (1992) *NATO ASI Ser. Ser. A 237*, 1−429.

Breton, J., Bylina, E. J., & Youvan, D. C. (1989) *Biochemistry 28*, 6423−6430.

Bylina, E. J., & Youvan, D. C. (1987) *Z. Naturforsch. 42C*, 769−774.

Bylina, E. J., & Youvan, D. C. (1988) *Proc. Natl. Acad. Sci., U.S.A. 85*, 7226−7230.

Bylina, E. J., Kowlaczkowski, S. V., Norris, J. R., & Youvan, D. C. (1990) *Biochemistry 29*, 6203−6210.

Callahan, P. M., & Cotton, T. M. (1987) *J. Am. Chem. Soc. 109*, 7001−7007.

Chang, C.-H., Tiede, D., Tang, J., Smith, U., Norris, J., & Schiffer, M. (1986) *FEBS Lett. 205*, 82−86.

Chirino, A. J., Lous, E. J., Huber, M., Allen, J. P., Schenck, C. C., Paddock, M. L., Feher, G., & Rees, D. C. (1994) *Biochemistry 33*, 4584−4593.

Cogdell, R. J., Parson, W. W., & Kerr, M. A. (1976) *Biochim. Biophys. Acta 430*, 83−93.

Deisenhofer, J., & Michel, H. (1989a) *Science 245*, 1463−1473.

Deisenhofer, J., & Michel, H. (1989b) *EMBO J. 8*, 2149−2169.

Deisenhofer, J., & Norris, J. R., Eds. (1993) *The Photosynthetic Reaction Center*, Vol. II, Academic Press: San Diego, CA.

Deisenhofer, J., Epp, O., Miki, R., Huber, R., & Michel, H. (1985) *Nature 339*, 618−624.

Deisenhofer, J., Epp, O., Sinning, I., & Michel, H. (1995) *J. Mol. Biol. 246*, 429−457.

Diers, J. R., & Bocian, D. F. (1994) *J. Phys. Chem. 98*, 12884−12892.

DiMagno, T. J., Bylina, E. J., Angerhofer, A., Youvan, D. C., & Norris, J. R. (1990) *Biochemistry 29*, 899−907.

Donohoe, R. J., Frank, H. A., & Bocian, D. F. (1988) *Photochem. Photobiol. 48*, 531−537.

El-Kabbani, O., Chang, C.-H., Tiede, D., Norris, J., & Schiffer, M. (1991) *Bichemistry 30*, 5361−5369.

Ermler, U., Fritzsch, G., Buchanan, S., & Michel, H. (1994) *Structure 2*, 925−936.

Feher, G. (1989) *Annu. Rev. Phys. Chem. 58*, 607−663.

Frank, H. A., & Cogdell, R. J. (1993) in *Carotenoids in Photosynthesis* (Young, A., & Britton, G., Eds.) Chapter 8, Springer-Verlag, Berlin.
Frank, H. A., Innes, J., Aldema, M., Neumann, R., & Schenck, C. C. (1993) *Photosynth. Res. 38*, 99−109.
Friesner, R. A., & Won, Y. (1989) *Biochim. Biophys. Acta 977*, 99−122.
Hammes, S. L., Mazzoli, L. T., Boxer, S. G., Gaul, D., & Schenck, C. C. (1990) *Proc. Natl. Acad. Sci. U.S.A. 87*, 5682−5686.
Huber, M., Lous, E. J., Isaacson, R. A., Feher, G., Gaul, D., & Schenck (1990) in *Reaction Centers of Photosynthetic Bacteria* (Michel-Beyerle, M. E., Ed.) pp 219−228, Springer-Verlag, Berlin.
Jones, M. R., Heer-Dawson, M., Mattioli, T. A., Hunter, C. N., & Robert, B. (1994) *FEBS Lett. 339*, 18−32.
Kirmaier, C., & Holten, D. (1987) *Photosynth. Res. 113*, 225−260.
Kirmaier, C., Holten, D., & Parson, W. W. (1985) *Biochim. Biophys. Acta 810*, 49−61.
Kirmaier, C., Holten, D., Bylina, E. J., & Youvan, D. C. (1988) *Proc. Natl. Acad. Sci. U.S.A. 85*, 7562−7566.
Kirmaier, C., Bylina, E. J., Youvan, D. C., & Holten, D. (1989) *Chem. Phys. Lett. 159*, 251−257.
Koyama, Y., Kito, M., Takii, T., Saiki, K., Tsukida, K., & Yamashita, J. (1982) *Biochim. Biophys. Acta 680*, 109−118.
Koyama, Y., Takii, T., Saiki, K., & Tsukida, K. (1983) *Photobiochem. Photobiophys. 5*, 139−150.
Koyama, Y., Umemoto, Y., & Akamatsu, A. (1986) *J. Mol. Struct. 146*, 273−287.
Krawczyk, S. (1989) *Biochim. Biophys. Acta 976*, 140−149.
Laporte, L., McDowell, L. M., Kirmaier, C., Schenck, C. C., & Holten, D. (1993) *Chem. Phys. 176*, 615−629.
Leonhard, M., & Mäntele, W. (1993) *Biochemistry 32*, 4532−4538.
Lutz, M. (1984) *Adv. Infrared Raman Spectrosc. 11*, 211−300.
Lutz, M., & Robert, B. (1988) in *Biological Applications of Raman Spectroscopy* (Spiro, T. G., Ed.) Vol. 3, pp 347−411, Wiley, New York.
Lutz, M., & Mäntele, W. (1991) in *Chlorophylls* (Scheer, H., Ed.) pp 855−902, CRC Press, Boca Raton, FL.
Lutz, M., Szponarski, W., Berger, G., Robert B., & Neumann, J.-M. (1988) *Biochim. Biophys. Acta 894*, 423−433.
Mattioli, T. A., Hoffman, A., Robert, B., Schrader, B., & Lutz, M. (1991) *Biochemistry 30*, 4648−4654.
Mattioli, T. M., Williams, J. C., Allen, J. P., & Robert, B. (1994) *Biochemistry 33*, 1636−1643.
McDowell, L. M., Kirmaier, C., & Holten, D. (1990) *Biochim. Biophys. Acta 1020*, 239−246.
McDowell, L. M., Kirmaier, C., & Holten, D. (1991a) *J. Phys. Chem. 95*, 3379−3383.
McDowell, L. M., Gaul, D., Kirmaier, C., Holten, D., & Schenck, C. C. (1991b) *Biochemistry 30*, 8315−8322.
McGann, W. J., & Frank, H. A. (1985) *Biochim. Biophys. Acta 807*, 101−109.
Myers, A. B., & Mathies, R. A. (1987) in *Biological Applications of Raman Spectroscopy* (Spiro, T. G., Ed.) Vol. 2, pp 1−58, Wiley, New York.
Nabedryk, E., Robles, S. J., Goldman, E., Youvan, D. C., & Breton, J. (1992) *Biochemistry 31*, 10852−10858.
Nabedryk, E., Allen, J. P., Taguchi, A. K. W., Williams, J. C., Woodbury, N. W., & Breton, J. (1993) *Biochemistry 32*, 13879−13885.
Nagarajan, V., Parson, W. W., Davis, D., & Schenck, C. C. (1993) *Biochemistry 32*, 12324−12336.
Peloquin, J. M., Violette, C. A., Frank, H. A., & Bocian, D. F. (1990a) *Biochemistry 29*, 4892−4898.
Peloquin, J. M., Bylina, E. J., Youvan, D. C., & Bocian, D. F. (1990b) *Biochemistry 29*, 8417−8424.
Peloquin, J. M., Bylina, E. J., Youvan, D. C., & Bocian, D. F. (1991) *Biochim. Biophys. Acta 1056*, 85−88.
Palaniappan, V., & Bocian, D. F. (1992) *NATO ASI Ser. Ser. A, 237*, 119−126.
Palaniappan., V., & Bocian, D. F. (1995) *J. Am. Chem. Soc. 117*, 3647−3648.
Palaniappan, V., Martin, P. C., Chynwat, V., Frank, H. A., & Bocian, D. F. (1993) *J. Am. Chem. Soc. 115*, 12035−12049.
Rafferty, C. N., & Clayton, R. K. (1979a) *Biochim. Biophys. Acta 545*, 106−121.
Rafferty, C. N., & Clayton, R. K. (1979b) *Biochim. Biophys. Acta 545*, 189−206.
Rautter, J., Lendzian, F., Lubitz, W., Wang, J., & Allen, J. P. (1994) *Biochemistry 33*, 12077−12084.
Robert, B. (1990) *Biochim. Biophys. Acta 1017*, 99−111.
Schenck, C. C., Gaul, D., Steffen, M., Boxer, S. G., McDowell, L., Kirmaier, C., & Holten, D. (1990) in *Reaction Centers of Photosynthetic Bacteria* (Michel-Beyerle, M. E., Ed.) pp 229−238, Springer-Verlag, Berlin.
Schilt, A. A. (1960) *J. Am. Chem. Soc. 82*, 3000−3005.
Shreve, A. P., Trautman, J. K., Owens, T. G., & Albrecht, A. C. (1991a) *Chem. Phys. Lett. 178*, 89−96.
Shreve, A. P., Trautman, J. K., Owens, T. G., & Albrecht, A. C. (1991b) *Chem. Phys. 154*, 171−178.
Shreve, A. P., Trautman, J. K., Frank, H. A., Owens, T. G., & Albrecht, A. C. (1991c) *Biochim. Biophys. Acta 1058*, 280−288.
Steffan, M., Lao, K., & Boxer, S. G. (1994) *Science 264*, 810−816.
Trautman, J. K., Shreve, A. P., Violette, C. A., Frank, H. A., Owens, T. G., & Albrecht, A. C. (1990) *Proc. Natl. Acad. Sci. U.S.A. 87*, 215−219.
Wachtveitl, J., Farchaus, J. W., Das, R., Lutz, M., Robert, B., & Mattioli, T. A. (1993) *Biochemistry 32*, 12875−12886.
Yeates, T. O., Komiya, H., Chirino, A., Rees, D. C., Allen, J. P., & Feher, G. (1988) *Proc. Natl. Acad. Sci. U.S.A. 85*, 7993−7997.

BI950677C